JOURNAL OF CATALYSIS 87, 196–209 (1984)

Cleavage of Diarylmethanes in the Presence of Zinc Halides

TIM J. FREDERICK[1] AND ALEXIS T. BELL

Materials and Molecular Research Division, Lawrence Berkeley Laboratory and Department of Chemical Engineering, University of California, Berkeley, California 94720

Received March 30, 1983; accepted December 2, 1983

A study has been conducted of the cleavage of aliphatic linkages between aromatic centers under the influence of zinc halide catalysts. The purpose of this work was to learn more about the chemistry occurring during the liquefaction of coal. 4-Hydroxydiphenylmethane (4-HDPM), 2,4,6-trimethyldiphenylmethane (TMDPM), and 1-benzylnaphthalene (1-BN) were used to simulate structural units present in coal. $ZnCl_2$, $ZnBr_2$, and ZnI_2 were used as catalysts. It was found that all of the zinc halides are active when converted to a Brönsted acid by interaction with either water or methanol. For a given catalyst, the reactivity of the reactants decreases in the order TMDPM > 4-HDPM > 1-BN. For a given reactant, the catalyst activity decreases in the order $ZnBr_2$ > $ZnCl_2$ > ZnI_2. Cleavage of the methylene linkage always occurred at the aryl group exhibiting the highest Brönsted basicity. The distribution of reaction products depended on reaction conditions, as well as on reactant and catalyst composition. The reaction kinetics for 4-HDPM, 1-BN, and TMPDPM can be described successfully in terms of a cabocation mechanism. Rate coefficients for each of the elementary steps in the sequence were determined by simulation of the experimental data.

INTRODUCTION

Aliphatic groups constitute one of the important linkages between aromatic and hydroaromatic clusters present in coal (*1–6*). During the liquefaction of coal, these linkages are cleaved. The rate at which this process occurs depends on the nature and degree of substitution of the aromatic centers to which the aliphatic groups are attached, and whether or not a catalyst is present. In the absence of a catalyst, it has been observed that at temperatures above 673 K dibenzyl-type linkages react more readily than diphenylmethane-type linkages, and that the reactivity of both is considerably greater than that of direct aryl–aryl linkages (*7*). The introduction of Lewis acid catalysts significantly accelerates the cleavage of aliphatic linkages. Tsuge and Tashiro have found that $AlCl_3$ catalyzes the total cleavage of many substituted forms of diarylmethane at temperatures as low as 373 K (*8*). Taylor and Bell have reported that $ZnCl_2$ catalyzes the cleavage of several substituted diphenylmethanes at 598 K (*9*). Their studies showed that, in general, substituted diphenylmethanes will cleave predominately at the substituted diphenyl group and to a lesser extent at the unsubstituted ring. Thus, for example, 4-hydroxydiphenylmethane was found to yield mostly phenol with a much lower yield of benzene.

This paper reports on the results of a study aimed at identifying the effects of zinc halide catalysts on the cleavage of the methylene linkages in diarylmethanes. 4-Hydroxydiphenylmethane, 2,4,6-trimethyldiphenylmethane, and 1-benzylnaphthalene were used to represent three of the commonly found structures present in coal. The reactions of these compounds were examined in the presence of $ZnCl_2$, $ZnBr_2$, and ZnI_2. The influence of additives such as water or alcohols was also considered. Based on the observed products and their distribution, a mechanism is proposed for the cleavage process. This mechanism is used to develop a theoretical model for the reac-

[1] Present address: Stauffer Chemical Co., Richmond, Calif. 94804.

0021-9517/84 $3.00

tion kinetics and to deduce rate coefficients for individual elementary processes.

EXPERIMENTAL

Reactions were carried out in a 300 cm^3, 316 stainless-steel, stirred autoclave (Autoclave Engineers, Inc. Model ABP-300) fitted with a glass liner. A 30-cm^3, stainless-steel vessel was connected to the gas inlet line and to the autoclave. This vessel was used to hold a solution of the reactant prior to its injection into the autoclave. The temperature of the autoclave contents was monitored using a sheathed thermocouple and the pressure within the autoclave was measured using a Bourdon gauge. Liquid samples were taken through a $\frac{1}{8}$-in. sampling tube which was cooled after emerging from the autoclave.

A run was begun by sieving the dried catalyst and placing 0.0050 mol of the 100/170 Tyler mesh (147–88 μm) cut in a glass liner, together with 50 ml of solvent. If an additive such as water or an alcohol was to be used, this was done by injecting the additive into the solvent using a microsyringe (Hamilton). This process was carried out in a nitrogen-purged dry box. The glass liner was quickly transferred to the autoclave, which was then sealed and flushed with nitrogen. The reactant was weighed in the dry box and dissolved in 20 ml of solvent. This solution was transferred to the reactant holding vessel, which was then flushed and pressurized with hydrogen. During the 40 min required to heat the autoclave to 598 K, the reactant holding vessel remained at room temperature. The reactant solution was then injected into the autoclave with hydrogen. The temperature of the autoclave dropped about 20 K at this point, but recovered to 598 K within 3 min. Liquid samples were taken during the next 3 to 6 hr as the reaction progressed.

Analysis of the liquid samples was carried out by gas chromatography using a 3 mm by 3 m, stainless-steel column packed with 5% OV-225 on Chromosorb P. Product identification was made using a Finnigan 4023 GC-MS and was verified by matching peak retention times with those of pure components.

4-Hydroxydiphenylmethane (Aldrich), 1-benzylnaphthalene (ICN Pharmaceuticals), and 2,4,6-trimethyldiphenylmethane were used as reactants. The last was synthesized from 1,3,5-trimethylbenzene and benzyl chloride and was purified by vacuum distillation and recrystallization from ethanol. The purified product melted at 308 to 309 K, in close agreement with the reported melting point (*10*). While 4-HDPM is known to be hygroscopic, preliminary experiments confirmed that drying of this reactant, prior to an experiment, was not required. Benzene (Mallinckrodt), cyclohexane (MCB), and ethylbenzene (MCB) were dried by refluxing under nitrogen in the presence of sodium. All reactants, solvents, and catalysts were stored in a dry box.

The catalysts, $ZnCl_2$(MCB), $ZnBr_2$ (MCB), and ZnI_2 (Fischer scientific), were dried for 88 hr at 383 K in a vacuum oven immediately prior to use. Water content of fresh and spent catalysts was measured by ^1H NMR using a Varian T-60 spectrometer. The zinc halide was dissolved in D_2O, and dimethyl sulfoxide was added as an internal standard. The relative areas of the H_2O to DMSO signal gave the water content of the sample, after correction for water in a blank DMSO–D_2O sample. The dried catalysts were found to retain the following amounts of water expressed as moles H_2O per mole ZnX_2: $ZnCl_2$, 0.027; $ZnBr_2$, 0.024; and ZnI_2, 0.020.

RESULTS

The reactions of 2,4,6-trimethyldiphenylmethane (TMDPM), 4-hydroxydiphenylmethane (4-HDPM), and 1-benzylnaphthalene (1-BN) were studied at 598 K using $ZnCl_2$, $ZnBr_2$, and ZnI_2 as catalysts. Benzene was used as the solvent, unless otherwise noted. Figures 1, 2, and 3 show the variation in reactant and product concentrations with time during the reactions of

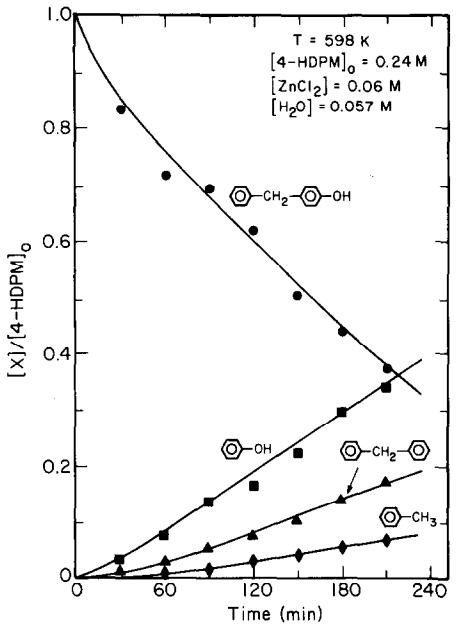

FIG. 1. Concentration versus time profiles observed for TMDPM.

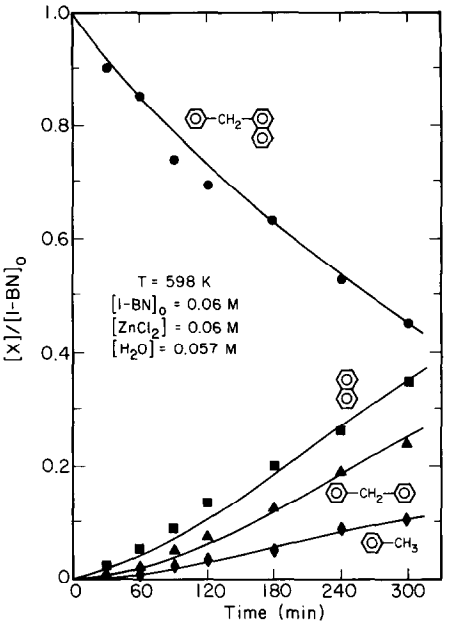

FIG. 3. Concentration versus time profiles observed for 1-BN.

TMDPM, 4-HDPM and 1-BN, respectively. Figure 1 shows that TMDPM cleaves at the substituted ring to yield 1,3,5-trimethylbenzene. The benzyl group released in the process either adds hydrogen to form toluene or reacts with the solvent, benzene, to form diphenylmethane. As may be seen in Figs. 2 and 3, 4-HDPM and 1-BN react in an analogous fashion. Thus, all three reactants undergo cleavage at the substituted ring to produce the substituted aromatic, diphenylmethane, and toluene.

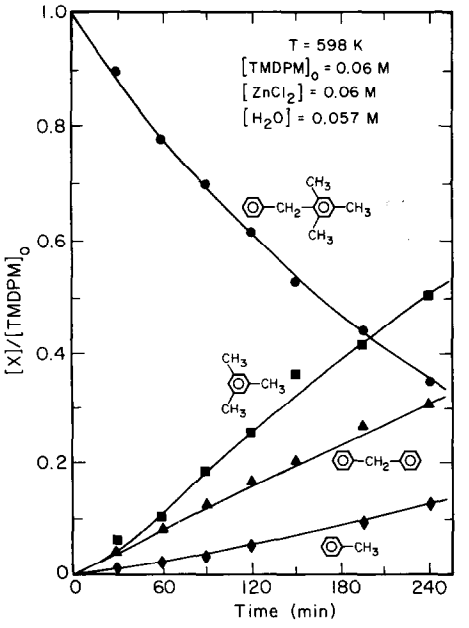

FIG. 2. Concentration versus time profiles observed for 4-HDPM.

As shown in Fig. 4, a plot of the logarithm of 4-HDPM concentration versus time is linear, indicating that the rate of 4-HDPM consumption is first order in the reactant concentration. Similar plots were also obtained for TMDPM and 1-BN. The slope of the line in Fig. 4 is defined as the apparent, first-order rate coefficient, k_a. As may be seen, the apparent rate coefficient decreases as the initial concentration increases from 0.06 to 0.24 M. Thus, while k_a is not an intrinsic rate coefficient, it is a useful characteristic of the rate of reaction.

For a given reactant, the magnitude of k_a is affected by catalyst composition and reaction conditions. A summary of these ef-

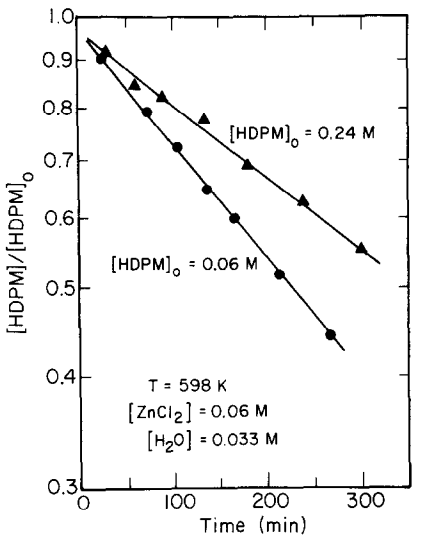

FIG. 4. Plot of log [HDPM]/[HDPM]$_0$ versus time.

fects is presented in Table 1. Consistent with the results in Fig. 4, k_a decreases when the initial reactant concentration is increased from 0.06 to 0.24 *M*. The magnitude of k_a increases, though, with increasing hydrogen pressure. Diluting the benzene with cyclohexane has no effect on k_a. Stirring speed also has no effect on k_a when $ZnBr_2$ or ZnI_2 is used as the catalyst. Both of these catalysts remain in the solid phase at reaction temperature, and, hence, the observed effect of stirring speed indicates that the rate of reaction is unaffected by liquid-phase mass transfer. In the case of $ZnCl_2$, the magnitude of k_a is seen to increase with increasing stirring speed. The reason for this behavior is that $ZnCl_2$ is molten at the temperatures used for these experiments, and the size of the melt droplet decreases with increasing stirring speed. It follows, therefore, that the reaction rate depends on the surface area of the $ZnCl_2$ droplets. Observation of the $ZnCl_2$ crystals under a microscope, following reaction, suggests that the surface area of the molten $ZnCl_2$ is roughly 10 times less than the surface area of the initially charged $ZnCl_2$ particles. As a consequence, it is concluded that the active surface area for $ZnCl_2$ is considerably lower than that for $ZnBr_2$ or ZnI_2.

Table 1 also shows that, for a given catalyst and set of reaction conditions, the values of k_a are comparable for 4-HDPM and TMDPM, but the value of k_a for 1-BN is three times smaller. Comparison of catalyst activities for a given reactant shows that activity decreases in the order $ZnBr_2 > ZnCl_2 > ZnI_2$.

Information on product yields is presented in Table 1. This characteristic is defined as the ratio of the rate of product formation to the rate of reactant consumption. It was observed that the yield of each product is independent of reactant conversion in all cases. Table 1 shows that the distribution of products obtained from each reactant depends on the catalyst composition and the reaction conditions. Toluene yields increase at the expense of diphenylmethane for the zinc halides in the order $ZnI_2 > ZnCl_2 > ZnBr_2$. Increasing the hydrogen pressure or diluting the benzene with cyclohexane increases the yield of toluene and decreases the yield of diphenylmethane. The toluene yield is also affected by the composition of the reactant and increases in the order TMDPM > 1-BN > 4-HDPM. The product distribution is not affected, though, by the reaction temperature or the initial concentration of the reactant.

The hydrogen pressure dependence of the rate of toluene formation can be obtained from the data in Table 1. The benzyl group alkylates the solvent to form diphenylmethane or undergoes hydrogenation to form toluene. Assuming a power-law dependence on hydrogen pressure and assuming the rate constant for diphenylmethane formation to be proportional to benzene concentration, the ratio of the toluene yield to DPM yield can be expressed as

$$\frac{Y_T}{Y_{DPM}} = \frac{k_2 P_{H_2}{}^{\alpha}}{k_3 B} \qquad (1)$$

where P_{H_2} is the hydrogen partial pressure, α is a dimensionless exponent, B is the benzene concentration, and Y_T and Y_{DPM} are the yields of toluene and diphenylmethane,

TABLE 1

Product Yields and Apparent Rate Coefficients for the Reactions of 4-HDPM, 1-BN, and TMPDPM[a]

Reactant	Catalyst	T (K)	Reactant conc. (M)	H_2 Pressure (atm)	Yield(%)			$k_a(s^{-1})$
					Phenol	Diphenyl-methane	Toluene	
4-HDPM	$ZnCl_2$	598	0.06	37	56	34	5	4.1×10^{-5}
	$ZnCl_2$	598	0.24	37	57	37	6	3.3×10^{-5}
	$ZnCl_2$	598	0.24	71	63	35	7.5	3.6×10^{-5}
	$ZnCl_2$	598	0.24	36[c]	82	32	13	4.2×10^{-5}
	$ZnBr_2$	598	0.24	44	67	45	8	9.0×10^{-5}
	$ZnBr_2$	598	0.24	37	62	18	13	1.6×10^{-5}
	$ZnBr_2$	598	0.24	73	57	19	24	1.7×10^{-5}
					Naphtha-lene	Diphenyl-methane	Toluene	
1-BN	$ZnCl_2$	598	0.06	44	66	54	14	1.5×10^{-5}
	$ZnCl_2$	598	0.24	49	57	35	15	9.4×10^{-6}
	$ZnCl_2$	598	0.06	65	61	40	20	2.1×10^{-5}
	$ZnBr_2$	598	0.06	44	70	63	7	3.4×10^{-5}
					Trimethyl benzene	Diphenyl-methane	Toluene	
TMDPM	$ZnCl_2$	598	0.06	10	70	48	12	3.6×10^{-5}
	$ZnCl_2$	598	0.06	20	75	49	17	3.9×10^{-5}
	$ZnCl_2$	598	0.06	44	78	49	24	4.1×10^{-5}
	$ZnCl_2$	598	0.06	70	87	50	36	5.1×10^{-5}
	$ZnCl_2$	598	0.24	44	82	49	27	2.5×10^{-5}
	$ZnCl_2$	598	0.06	43[c]	81	31	49	4.2×10^{-5}
	$ZnCl_2$	598	0.06	44[d]	83	51	24	5.4×10^{-5}
	$ZnCl_2$	579	0.06	39	75	50	25	1.7×10^{-5}
	$ZnCl_2$	618	0.06	48	83	59	24	9.2×10^{-5}

[a] Unless otherwise noted, all reactions were carried out in benzene using a 0.06 M loading of ZnX_2 and a stirring speed of 600 rpm.
[b] Defined at moles of product obtained per mole of reactant consumed.
[c] The solvent for this experiment was a 50/50 molar mixture of cyclohexane and benzene.
[d] The stirring speed for this experiment was 1200 rpm.

respectively. The rate coefficients refer to the reactions that form the respective products and will be explained further in the Discussion. A plot of log (Y_T/Y_{DPM}) versus log P_{H_2} is shown in Fig. 5. The slope of this line gives a value for α very close to 0.5 for each of the three reactants. This indicates that the rate of toluene formation is half-order in hydrogen pressure.

In addition to forming phenol, diphenylmethane, and toluene, 4-HDPM was observed to isomerize to 2-hydroxydiphenylmethane, in yields of about 15%. The rate of cleavage of 2-HDPM is somewhat slower than 4-HDPM but the products are the same (*8*). Since the ratio of 2-HDPM to 4-HDPM was small throughout the reaction, both isomers were lumped together for the purpose of analyzing the reaction kinetics. The reaction of 4-HDPM could then be treated in a manner analogous to that for TMDPM and 1-BN where rearrangement was not observed.

The product yields reported in Table 1 do not account for all of the reactant consumed. The fraction of the converted reactant not accounted for was 40% for 4-HDPM and 1-BN and 20% for TMDPM. Analysis of the gas inside the autoclave after reaction showed no products. A high-molecular-weight residue was found, following distillation of the solution obtained after the reaction of 4-HDPM. Gas chromatographic analysis of the residue could not be obtained, since the constituents of the residue were too heavy to elute. Infrared

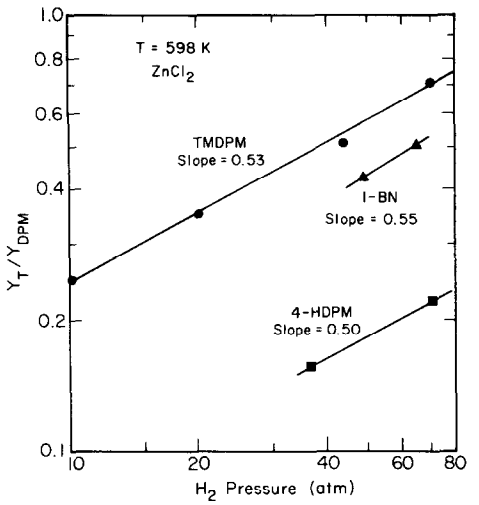

FIG. 5. Plot of $\log(Y_T/Y_{DPM})$ versus $\log P_{H_2}$.

and uv analyses indicated, though, that the residue contains phenolics. It is very likely that the residue is formed via Scholl condensation of 4-HDPM. This process is readily catalyzed by Lewis acids and has been observed to occur for dihydronaphthalene in the presence of $ZnCl_2$ (*11*). The fact that the combined yield of toluene and DPM is lower than the yield of phenol indicates the occurrence of a reaction consuming benzyl groups. It is quite conceivable that the unaccounted for benzyl groups are attached to the high-molecular-weight residue. In the case of TMDPM and 1-BN, the residue appears to be formed strictly from the reactant, since the yields of toluene plus diphenylmethane are very close to that of trimethylbenzene or naphthalene for these reactants.

To determine whether cleavage of the aliphatic linkage might also occur at the phenyl ring, experiments were carried out using ethylbenzene as the solvent. No ethyl analogs of the reactants were formed, indicating that cleavage does not occur at the phenyl ring. The products observed were the same as those produced in benzene except for the appearance of two isomers of ethyldiphenylmethane and the absence of diphenylmethane.

The addition of water to the catalyst was found to have a very strong effect on the apparent rate coefficient. Figures 6 and 7 show that for many combinations of reactant and catalyst, k_a increases with increasing water addition up to the point where $H_2O/ZnCl_2 = 1.0$. At higher ratios of water to $ZnCl_2$, k_a decreases sharply form its maximum value. In contrast to its effect on k_a, the addition of water had no effect on the observed product distribution. Extrapolation of the data obtained from $H_2O/ZnX_2 < 1$ to $H_2O/ZnX_2 = 0$ suggests that anhydrous $ZnCl_2$ and ZnI_2 are not very active. This could not be verified because water could not be totally excluded from the autoclave. The water to zinc halide ratio measured after reaction for the case where no water had been added was 0.6. This level is significantly higher than that for the catalyst itself (~0.02) probably due to the introduction of trace amounts of water with the hydrogen which was not dried.

The effect of adding methanol to $ZnCl_2$ is identical to that of adding water, as shown in Fig. 7. The product distribution obtained from TMDPM was also found to be the same whether water or methanol was added

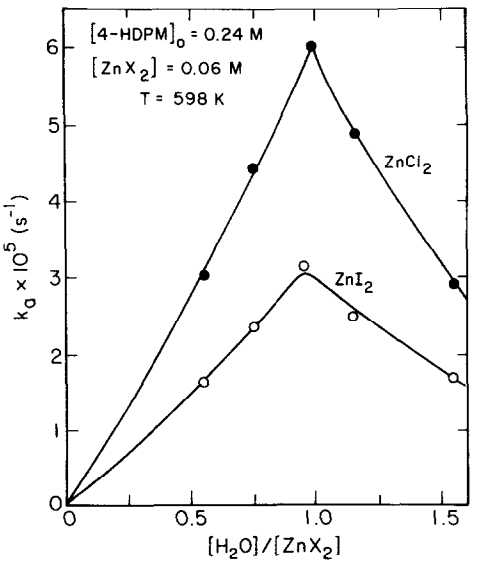

FIG. 6. Effect of $[H_2O]/[ZnX_2]$ on k_a for the reaction of 4-HDPM.

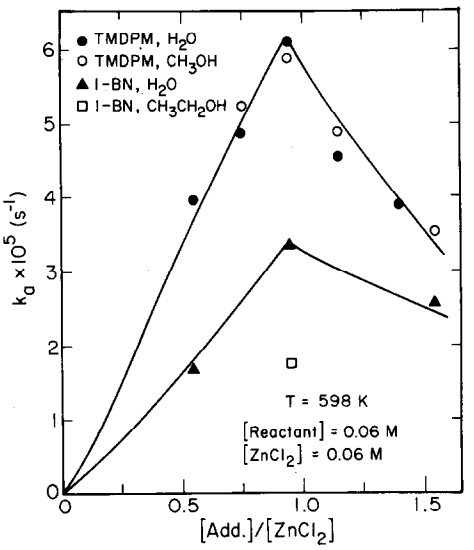

FIG. 7. Effect of [Add.]/[$ZnCl_2$] on k_a for the reactions of TMDPM and 1-BN.

to the catalyst, and no evidence was observed for products derived from methanol. The effect of ethanol, though, was different. Figure 7 shows that the value of k_a for 1-BN is the same when $H_2O/ZnCl_2 = 0.55$ and $(H_2O + CH_3CH_2OH)/ZnCl_2 = 0.95$ [i.e., $CH_3CH_2OH/ZnCl_2 = 0.4$]. Thus, ethanol addition appears not to have an effect on the activity of $ZnCl_2$. Moreover, in contrast to methanol, ethanol reacts slowly with the aromatics present in solution to form ethylbenzene, ethylnaphthalene, ethyldiphenylmethane, and ethyl-(benzylnaphthalene).

DISCUSSION

Active Form of the Catalyst

The data presented in Figs. 6 and 7 indicate that the addition of water to $ZnCl_2$ and ZnI_2 enhances the activity of these catalysts up to the point where $H_2O/ZnCl_2 = 1.0$, and suggests that the active form of the catalyst is a hydrate of the zinc halide. Several authors have proposed that zinc halides readily form mono-and dihydrates (*11–13*). The fact that k_a reaches a sharp maximum at about $H_2O/ZnCl_2 = 1$ suggests that the monohydrate is more active catalytically than the dihydrate. This is consistent with the fact that the acidity of $ZnCl_2$ decreases rapidly as hydration increases (*14*). It is of interest to note that Beishline *et al.* (*11*) observed a similar maximum in the activity of $ZnCl_2$ for Scholl condensation of 1,2-dihydronaphthalene. These authors propose that the active form of the catalyst is the monohydrate.

Reaction Mechanism

The cleavage of diarylmethanes under the influence of zinc halide catalysts can be interpreted on the basis of the mechanism presented in Fig. 8. While the reaction sequence shown in specifically for 4-HDPM and $ZnCl_2$, the same mechanism is assumed to be operative for TMDPM and 1-BN. Based on the results presented in Fig. 6, the active form of the catalyst is assumed to be the monohydrate of zinc chloride, $H_2O \cdot ZnCl_2$. The formation of a dihydrate, $(H_2O)_2 \cdot ZnCl_2$, is also shown, but this form is taken to be inactive. In reaction 1, $H_2O \cdot ZnCl_2$ protonates the phenolic ring of 4-HDPM, since this ring is more basic than the unsubstituted phenyl ring (*15*). This re-

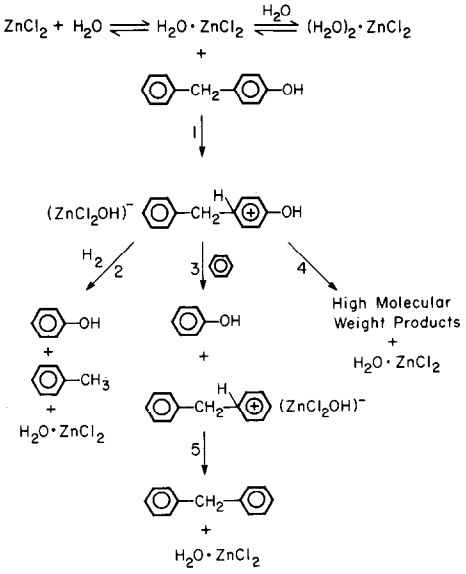

FIG. 8. Mechanism for the reaction of 4-HDPM.

action is analogous to the protonation of aromatic compounds with $HCl \cdot AlCl_3$ (*16*), $HF \cdot SbF_5$ (*17*), and $HSO_3F \cdot SbF_5$ (*18*) reported previously. The protonated reactant can then form products via three pathways. The participation of H_2 in reaction 2 leads to the formation of phenol and toluene. Reaction 3 involves the solvent, benzene, and results in cleavage of the methylene linkage with the release of phenol and protonated diphenylmethane. The latter product forms diphenylmethane in reaction 5. Reaction 4, on the other hand, results in the formation of Scholl condensation products through the interaction of the protonated 4-HDPM with various aromatic components present in the reacting solution. The participation of $H_2O \cdot ZnCl_2$ in producing such products from dihydronaphthalene has been observed recently (*11*). It is noted that reactions 2 through 4 are envisaged to occur without the intermediate formation of a benzyl cation. If benzyl cations were intermediates in the formation of toluene and diphenylmethane, then the ratio of these products would not be expected to depend on the nature of the reactant, as was observed in the present experiments (see Table 1).

Analysis of the Reaction Kinetics

The mechanism presented in Fig. 8 can be used to represent the kinetics of the reactions of diarylmethanes. To do so, the autoclave is modeled as a well-stirred, isothermal, batch reactor. The concentration of each species in the reactor can be expressed by the mass balances in Eqs. (2)–(8).

$$\frac{dH}{dt} = -k_1 Z_1 H \tag{2}$$

$$\frac{dZ_1}{dt} = -k_1 Z_1 H + k_2 P_{H_2}^{1/2} I_1 + k_5 I_2 + k_4 I_1 \tag{3}$$

$$\frac{dI_1}{dt} = k_1 Z_1 H - k_2 P_{H_2}^{1/2} I_1 - k_3 B I_1 - k_4 I_1 \tag{4}$$

$$\frac{dI_2}{dt} = k_3 B I_1 - k_5 I_2 \tag{5}$$

$$\frac{dP}{dt} = k_2 P_{H_2}^{1/2} I_1 + k_3 B I_1 \tag{6}$$

$$\frac{dT}{dt} = k_2 P_{H_2}^{1/2} I_1 \tag{7}$$

$$\frac{dD}{dt} = k_3 B I_1 \tag{8}$$

where

B = concentration of benzene, M
H = concentration of 4-HDPM, M
Z_0 = concentration of $ZnCl_2$, M
Z_1 = concentration of $H_2O \cdot ZnCl_2$, M
Z_2 = concentration of $(H_2O)_2 \cdot ZnCl_2$, M
W = concentration of water, M
I_1 = concentration of protonated 4-HDPM, M
I_2 = concentration of protonated DPM, M
P = concentration of phenol, M
T = concentration of toluene, M
D = concentration of diphenylmethane, M

The subscripts on the rate coefficients refer to the number of the reaction in the mechanism in Fig. 8. The species concentrations in these equations are based on the volume of solution. The dispersion of the catalyst is not included explicitly because the surface area of the molten zinc chloride could not be determined. The dispersion is implicit in the value of k_1 so that the values determined for this rate coefficient are a function of the dispersion.

The water–zinc chloride system was assumed to be at equilibrium throughout the reaction. The concentrations of $ZnCl_2$, H_2O, $H_2O \cdot ZnCl_2$, and $(H_2O)_2 \cdot ZnCl_2$ are given by Eqs. (9) and (10)

$$K_1 = \frac{Z_1}{Z_0 W} \tag{9}$$

$$K_2 = \frac{Z_2}{Z_1 W} \tag{10}$$

where K_1 and K_2 are the equilibrium con-

stants for forming the mono- and dihydrates of $ZnCl_2$. The concentration of water is given by

$$W = W_0 - Z_1 - 2Z_2 - I_1 - I_2 \quad (11)$$

where W_0 is the initial concentration of H_2O.

The initial conditions for Eqs. 2–11, at $t = 0$ are given by

$$H = H_0 \qquad P = 0$$
$$I_1 = 0 \qquad D = 0$$
$$I_2 = 0 \qquad T = 0$$

H_0 is the initial reactant concentration. The initial concentrations of Z_0, Z_1, Z_2, and W are calculated from Eqs. (9)–(11) and the $ZnCl_2$ mass balance using the initial loadings of $ZnCl_2$ and water.

Equations (2) through (8) were integrated using a Runge–Kutta–Gill routine (*19*). The concentration versus time curves determined for a given set of rate coefficients were then compared with the concentrations profiles observed experimentally. If the agreement between theory and experiment was poor, a new set of rate coefficients was chosen to better fit the experimental results. A Sequential Simplex algorithm was used to obtain the best set of rate coefficients (*20*).

The model as written involves seven parameters—five rate coefficients and two equilibrium coefficients. When all seven parameters were adjusted simultaneously, it was not possible to determine unique values for each parameter. This situation was avoided by reducing the number of parameters adjusted at one time. The following procedure was used for this purpose. The data for experiments at low water levels ($H_2O/ZnCl_2 < 0.75$) were simulated first. Since it can be assumed that all of the water in these experiments is bound up in the monohydrate, the magnitude of the equilibrium coefficients is unimportant. The five rate coefficients appearing in Eqs. (2) through (8) can be reduced to a set of three by considering the reactions of the protonated intermediate. Since reactions 2 through 4 are all first-order in the concentration of the intermediate, Eq. (4) can be rewritten as

$$\frac{dI_1}{dt} = k_1 Z_1 H - k_p I_1 \quad (12)$$

where

$$k_p = k_2 P_{H_2}^{1/2} + k_3 C_B + k_4.$$

Thus, for experiments at low water levels, the three adjustable parameters become k_1, k_p, and k_5. The actual rate coefficients are then retrieved from the following relations:

$$k_2 P_{H_2}^{1/2} = k_p Y_{TB} \quad (13)$$

$$k_3 C_B = k_p Y_{DPM} \quad (14)$$

$$k_4 = k_p - (k_2 P_{H_2}^{1/2} + k_3 C_B). \quad (15)$$

Equations (13) and (14) emerge from the definition of product yields. Once the rate coefficients had been determined by fitting the experiments carried out using low water levels, the equilibrium constants could be obtained by fitting experiments carried out at high water levels ($H_2O/ZnCl_2 < 1.1$).

The rate coefficients obtained by fitting the predicted concentration versus time curves to those observed experimentally are given in Table 2. For a given catalyst, the values for k_1 follow the same order as the apparent rate coefficients. The values for k_1 for TMDPM and 4-HDPM are almost equal, while that for 1-BN is only one-half of these values. The rate coefficients for toluene and DPM formation fall in the same relative order as the observed yields. The rate coefficient for toluene formation, k_2, decreases in the order TMDPM > 1-BM > 4-HDPM. The rate coefficient for decomposition of protonated DPM, k_5, is equal for the three reactants, as would be expected.

The apparent, first-order dependence of the rate of reactant consumption can be explained in terms of the proposed model for the reaction kinetics. For this purpose, it is assumed that the concentrations of the two intermediates can be described by ex-

TABLE 2

Rate Coefficients Used for the Simulation of the Concentration Versus Time Profiles Observed at 598 K

Reactant	Catalyst	k_1(cm³/mol · s)	k_2(1/s · atm$^{1/2}$)	k_3(cm³/mol · s)	k_4(s^{-1})	k_5(s^{-1})
TMDPM	$ZnCl_2$	1.4	2.7×10^{-5}	3.2×10^{-2}	2.0×10^{-4}	5.9×10^{-4}
1-BN	$ZnCl_2$	7.8×10^{-1}	2.1×10^{-5}	2.4×10^{-2}	2.8×10^{-4}	6.1×10^{-5}
4-HDPM	$ZnCl_2$	1.6	4.4×10^{-5}	1.1×10^{-2}	3.8×10^{-4}	6.6×10^{-5}
4-HDPM	$ZnBr_2$	5.7	5.6×10^{-5}	1.8×10^{-2}	2.1×10^{-4}	4.2×10^{-5}
4-HDPM	ZnI_2	1.1	3.9×10^{-5}	3.3×10^{-3}	1.1×10^{-4}	5.6×10^{-5}

pressions deduced from Eqs. (6) and (7), following the imposition of the steady-state assumption. Substitution of these experiments into Eq. (3) gives

$$\frac{dH}{dt} = \frac{-k_1 H Z_1}{1 + (1 + k_3 C_B/k_5) k_1 H/k_p} \quad (16)$$

where Z_1 is the initial concentration of $H_2O \cdot ZnCl_2$. For most reaction conditions investigated in this work, the rate coefficients and concentrations are found to satisfy the inequality

$$(1 + k_3 C_B/k_5) \frac{k_1 H}{k_p} < 1 \quad (17)$$

so that the rate of reactant disappearance is approximated by

$$\frac{dH}{dt} = -k_1 Z_1 H = -k_a H. \quad (18)$$

This approximation is equivalent to assuming that reaction 1 is rate-limiting. A first-order dependence on reactant concentration is predicted and is found experimentally as shown in Fig. 4. Neither hydrogen pressure nor solvent composition has any effect in this approximation, because these variables affect reactions which occur after the slow step in the mechanism. The inequality in Eq. (17) starts to break down as the reactant concentration increases. As H increases, the second term in the denominator of Eq. 16 becomes significant compared to 1, and the apparent rate coefficient decreases. This explains the response of the apparent rate coefficient to changes in the initial reactant concentration reported in Fig. 4 and Table 1.

The results presented in Table 2 indicate that the value of k_1 for the reaction of 4-HDPM depends on the catalyst composition and decreases in the order $ZnBr_2 > ZnCl_2$ ZnI_2. This sequence stands in contrast with that which would be expected on the basis of decreasing acidity, namely $ZnCl_2 > ZnBr_2 > ZnI_2$. The fact that k_1 for $ZnCl_2$ is smaller than for $ZnBr_2$ can be explained in the following manner. It will be recalled that k_1, as used in the present model, represents the product of the intrinsic rate coefficient for reaction 1 and the catalyst dispersion. The dispersion of all three zinc halides prior to reaction is the same. For $ZnBr_2$ and ZnI_2, the initial dispersion is retained under reaction conditions, since these catalysts do not melt. Zinc chloride, on the other hand, melts under reaction conditions and forms droplets that are about 10-fold larger in diameter than the initial particles placed in the autoclave. As a consequence, the active surface area for $ZnCl_2$ is a factor of ten lower than that for $ZnBr_2$ or ZnI_2. If this fact is taken into account, it can readily be seen that the sequence of values for k_1 follows the order of relative catalyst acidity.

In Table 1 it was shown that the distribution of final products obtained from a given reactant depends on the catalyst composition. It is aparent from Table 2 that the rate coefficients for reaction 2, which produces toluene, are nearly the same for all three catalysts. Consequently, the observed differences in selectivity arise primarily from differences in the values of k_3 and k_4. The values for k_3 decrease in the order $ZnBr_2 >$

TABLE 3

Rate Coefficients for TMDPM

	k_1	k_2	k_3	k_4	k_5
Preexponential factor	8.0×10^{12}(cm³/mol · s)	1.7(1/s · atm$^{1/2}$)	1.3×10^5(cm³/mol · s)	1.7×10^1(s^{-1})	1.2×10^4(s^{-1})
Activation energy (kcal/mol)	34.9	13.1	18.1	8.0	20.0

$ZnCl_2 > ZnI_2$, and the values for k_4 decrease in the order $ZnCl_2 > ZnBr_2 > ZnI_2$.

Values of the rate coefficients from the elementary processes involved in the reaction of TMDPM in the presence of $ZnCl_2$ are given in Table 3. Activation energies for each process are also given. Reaction 1 exhibits the highest activation energy, 35 kcal/mol. The activation energies for reactions 2 through 4 are significantly smaller. It is for this reason that the product yields presented in Table 1 are not strongly dependent on temperature in the range of 573 to 623 K. The high activation energy found for reaction 5, 20 kcal/mol, indicates that the removal of the proton attached to diphenylmethane is an energy-intensive process.

Values for the equilibrium constants, K_1 and K_2, were obtained by fitting the predicted concentration versus time profiles to those observed experimentally for cases where $H_2O/ZnCl_2$ exceeded unity. The rate coefficients used for this phase of the analysis were the same as those deduced by obtaining a coincidence between theory and experiment for reactions where $H_2O/ZnCl_2 < 1.0$. The quality of the final theoretical representation can be judged by inspection of Figs. 1, 2, 3, 6, and 7. The solid curve in each of these figures gives the theoretical prediction. It is apparent that the proposed theoretical model does provide a good description of the experimental results. This is particularly evident in Figs. 1, 2, and 3 where the data were not used in the process of determining either the rate coefficients or the equilibrium constants.

The equilibrium constants obtained by fitting the experimentally observed concentration versus time curves for the three diarylmethanes are given in Table 4. The values of K_1 determined for $ZnCl_2$ show relatively little variation from reactant to reactant. The values of K_1 determined from experiments conducted with 4-HDPM and TMDPM are nearly the same. The magnitude of K_1 for the experiment carried out with 1-BN is a factor of 10 smaller. No reason can be given for this. The magnitudes of K_1 and K_2 are consistent with the earlier assumption that virtually all the water is tied up as $H_2O \cdot ZnCl_2$ at low water levels. Thus, for example, at $H_2O/ZnCl_2 = 0.75$, 96% of the water is in the form of $H_2O \cdot ZnCl_2$, 3.8% is in the form of $(H_2O)_2 \cdot ZnCl_2$, and 0.2% is present as free water.

The values of the equilibrium constants reported in Table 4 are consistent with the properties of zinc halides. The large value for K_1 is expected due to the very hygroscopic nature of $ZnCl_2$, while a lower value for K_2 results from the less hygroscopic and less Lewis acidic nature of hydrated $ZnCl_2$. $ZnCl_2$ is more hygroscopic than ZnI_2 and, correspondingly, K_1 is smaller than ZnI_2.

TABLE 4

Equilibrium Constants for ZnX_2 and H_2O at 598 K

Reactant	Catalyst	K_1(cm³/mol)	K_2(cm³/mol)
4-HDPM	$ZnCl_2$	3.2×10^7	2.0×10^5
TMDPM	$ZnCl_2$	2.6×10^7	1.9×10^5
1-BN	$ZnCl_2$	2.1×10^7	1.7×10^4
4-HDPM	ZnI_2	1.0×10^7	1.8×10^5

The less acidic nature of zinc iodide is also the reason for the lower rate coefficient for protonation in reaction 1 and the lower apparent rate coefficient for ZnI_2 in these reactions. The values of the second equilibrium constant are roughly equal for $ZnCl_2$ and ZnI_2. The identity of the halide attached to the zinc apparently has little effect on the ability of the monohydrate to add a second molecule of water.

The structure of the hydrates is not known but the equilibrium constants seem to be consistent with a structural model proposed for several Lewis acid complexes. In the systems BF_3–H_2O (*21, 22*), BF_3–CH_3OH (*23, 24*), and $SbCl_5$–H_2O (*25*), the first additive molecule complexes to the metal via an interaction of the lone-pair electrons on the oxygen atom of the additive with the metal. The second additive molecule does not attach to the metal but, rather, hydrogen bonds to the acidic proton of the first additive molecule to produce a chain-like structure. This type of structure would be consistent with the equilibrium constants found in this study. The second water molecule is presumed to be attached not to the zinc but to the first water molecule and, therefore, the effect of the halide on the acidity of the hydrogen atoms should be diminished for higher hydrates.

Gillespie and Hartman (*21–23*) have found that the systems H_2O/BF_3 and CH_3OH/BF_3 form similar, acidic complexes. Their results are in agreement with those reported here, which indicate that the $CH_3OH/ZnCl_2$ system exhibits catalytic properties very similar to those of $H_2O/ZnCl_2$.

The behavior of ethanol does not mimic the behavior of water or methanol, even though ethanol will also complex strongly with $ZnCl_2$ (*26*). Instead of cleaving at the O–H bond to yield the acidic proton, ethanol cleaves at the O–C bond to alkylate the aromatics in solution. Alkylation was not observed for methanol but this is consistent with the order of reactivity for Friedel–Crafts alkylation where the reactivities increase in the order methanol < ethanol < propanol (*27*). Ethanol reacts slowly under these reaction conditions while methanol is unreactive. Higher alcohols should show no catalytic effect in the alcohol form because they would alkylate instead of protonating the aromatics. Higher alcohols would alkylate more rapidly than ethanol and produce water as a by-product. This water would form the catalytically active $ZnCl_2$ hydrate and accelerate the reaction. Therefore, it is expected that an increase in reaction rate would be observed with higher alcohols if they reacted rapidly to produce water.

CONCLUSIONS

The present studies have shown that $ZnCl_2$, $ZnBr_2$, and ZnI_2, promoted with either water or methanol, are active catalysts for the cleavage of the methylene linkage in diarylmethanes. The additive converts the Lewis acid zinc halide into a Brönsted acid. Maximum catalyst activity is achieved at an additive-to-zinc halide ratio of unity. Above this level, hydrogen bonding between the protons of the Brönsted acid and the additive reduces the catalyst activity. In contrast to methanol, ethanol is not an effective promoter. Instead of producing a stable Brönsted acid, ethanol rapidly alkylates any aromatic centers present in the reaction system.

The rate of cleavage of methylene bridges between aryl centers is influenced by both reactant and the catalyst composition. For a given catalyst, the reactivity of the diphenylmethanes studied decreases in the order TMDPM $\gtrsim$ 4-HDPM > 1-BN. For a given reactant, the catalyst activity decreases in the order $ZnBr_2$ > $ZnCl_2$ > ZnI_2.

In all cases examined, cleavage of the methylene linkage occurs at the aryl group exhibiting the highest Brönsted basicity. Thus, for example, in benzene solution, 4-HDPM produces phenol, diphenylmethane,

and toluene. The selectivity between diphenylmethane and toluene is a function of H_2 pressure, solvent composition, reactant structure, and catalyst composition. For a given reactant–catalyst pair, the selectivity toward toluene is enhanced at high H_2 pressures and in a nonaromatic solvent. Under comparable reaction conditions using a given reactant, the toluene selectivity decreases in the order $ZnI_2 > ZnBr_2 > ZnCl_2$. Toluene selectivity decreases in the order TMDPM > 1-BN > 4-HDPM when examined for a fixed catalyst composition and set of reaction conditions.

The reaction kinetics for 4-HDPM, 1-BN, and TMDPM can be described in terms of a carbocation mechanism. Reaction is initiated by protonation of the reactant. The carbocation thus formed reacts with either H_2, solvent, or additional reactant to produce the final products observed. This picture of the reaction sequence provides an accurate description of the kinetics and permits deduction of the rate parameters for each elementary step.

The results of this investigation suggest that one of the reasons why zinc halides promote the liquefaction of coal is that these compounds catalyze the cleavage of aliphatic linkages. Since large amounts of water are released during liquefaction due to the cleavage of ether linkages (*28, 29*), promotion of the catalyst can be achieved without intentional addition of water or methanol. By choosing the catalyst composition and reaction conditions appropriately, it should be possible to assure that benzylic groups released during the cleavage of aliphatic linkages are terminated by reaction with hydrogen rather than by reaction with aromatic centers.

ACKNOWLEDGMENT

This work was supported by the Division of Chemical Sciences, Office of the Basic Energy Sciences, U.S. Department of Energy under Contract DE-AC03-76SF00098.

REFERENCES

1. Heredy, L. A., and Neuworth, M. B., *Fuel* **41,** 221 (1962).
2. Heredy, L. A., Kostyo, A. E., and Neuworth, M. B., *Fuel* **44,** 125 (1965).
3. Heredy, L. A., Kostyo, A. E., and Neuworth, M. B., *Adv. Chem. Ser.* **55,** 493 (1966).
4. Kuhlmann, E., Boerwinkle, E., and Orchin, M., *Fuel* **60,** 1002 (1981).
5. Huston, J. L., Scott, R. G., and Studier, M. H., *Fuel* **55,** 281 (1976).
6. Franz, J. A. Morrey, J. R., Tingey, G. L., Skiens, W. E., Pugmire, R. J., and Grant, D. M., *Fuel* **56,** 366 (1977).
7. Benjamin, B. M., Raaen, V. F., Maupin, P. L., Brown, L. L., and Collins, C. J., *Fuel* **57,** 269 (1978).
8. Tsuge, O., and Tashiro, M., *Bull. Japan Chem. Soc.* **38,** 184 (1965).
9. Taylor, N. D., and Bell, A. T., *Fuel* **59,** 499 (1980).
10. Bredereck, H., Lehmann, G., Schonfeld, C., and Fritzsche, E., *Chem. Ber.* **72,** 1414 (1939).
11. Beishline, R. R., Gould, B., Walker, E. B., Stuart, D. K., Schultzski, J., Shigley, J. K., Calvert, K., Dalling, D. K., and Anderson, L. L., *J. Org. Chem.* **47,** 1668 (1982).
12. Zielke, C. W., Struck, R. T., Evans, J. M., Constanza, C. P., and Gorin, E., *Ind. Eng. Chem. Proc. Des. Dev.* **5,** 151 (1966).
13. Olah, G. A., "Friedel-Crafts Chemistry." Wiley, New York, 1973.
14. Duffy, J. A., and Ingram, M. D., *Inorg. Chem.* **1,** 2988 (1977); **12,** 2798 (1978).
15. Olah, G. A., Staral, J. S., Asencio, G., Liang, G., Forsyth, D. A., and Mateescu, G. D., *J. Amer. Chem. Soc.* **100,** 6299 (1978).
16. Okami, Y., Otani, N., Katoh, D., Hamanaka, S., and Ogawa, M., *Bull. Chem. Soc. Japan* **46,** 180 (1973).
17. Olah, G. A., Staral, J. S., Asencio, G., Liang, G., Forsyth, D. A., and Mateescu, G. D., *J. Amer. Chem. Soc.* **100,** 6299 (1978).
18. Olah, G. A., Scholsberg, R. H., Porter, R. D., Mo, Y. K., Kelly, D. P., and Mateescu, G. D., *J. Amer. Chem. Soc.* **94,** 2034 (1972).
19. Lapidus, L., "Digital Computation," p. 89. McGraw-Hill, New York, 1962.
20. Beveridge, G. S., and Schechter, R. S., "Optimization: Theory and Practice," p. 367. McGraw-Hill, New York, 1970.
21. Gillespie, R. J., and Hartman, J. S., *Canad. J. Chem.* **45,** 859 (1967).
22. Gillespie, R. J., and Hartman, J. S., *Acta Chem. Scand. A* **28,** 929 (1974).
23. Gillespie, R. J., and Hartman, J. S., *Canad. J. Chem.* **45,** 2243 (1967).

24. Servis, K. L., and Jao, L., *J. Phys. Chem.* **76,** 329 (1972).
25. Bernander, L., and Olofsson, G., *Acta Chem. Scand.* **27,** 1034 (1973).
26. Kuchkarov, A. B., *J. Gen. Chem. USSR* **22,** 1171 (1952).
27. Schriessheim, A., *in* "Friedel-Crafts and Related Reactions" (G. A. Olah, ed.), Vol. 2, pp. 477–595. Wiley, New York, 1964.
28. Whitehurst, D. D., ed. "Coal Liquefaction Fundamentals," ACS Symposium Series 139, 1980.
29. Grens, E. A., Hershkowitz, F., Holten, R. R., Shinn, J. H., and Vermeulen, T., *Ind. Eng. Chem. Proc. Des. Dev.* **19,** 396 (1980).